PHYSICAL REVIEW B VOLUME 38, NUMBER 9 15 SEPTEMBER 1988-II

Resonant Raman-active acoustic phonons in ion-implanted GaAs

M. Holtz* and R. Zallen
Department of Physics, Virginia Tech, Blacksburg, Virginia 24061

O. Brafman
Department of Physics and Solid State Institute, Technion-Israel Institute of Technology, Haifa, Israel

(Received 14 March 1988)

We have observed a new, strong feature at 47 cm^{-1} in the first-order Raman spectrum of ion-implanted GaAs, prior to any anneal. It is not present in the Raman spectrum of either amorphous or single-crystal GaAs. The peak is strong between excitation photon energies ~ 1.5 and 2.2 eV. Above 2.2 eV it is masked by the Raman spectrum of the amorphous GaAs component of the mixed microcrystalline-amorphous system. Its frequency and line shape are not dependent upon implant species or energy. The photon-energy dependence of the intensity of the amorphous GaAs component of the Raman spectrum is found to be completely accounted for by the photon-energy dependence of the optical penetration depth over the full range studied (1.55–2.71 eV). This then serves as an internal intensity standard for our measurements, permitting us to separate scattering efficiencies from mere scattering volume effects. The longitudinal-optical phonon of the microcrystalline remnant resonates near the E_1 interband transition peak in the electronic density of states, consistent with a feature corresponding to a Raman-active crystal phonon. However, the new feature at 47 cm^{-1} is observed to resonate strongly at an energy near the E_0 and $E_0+\Delta_0$ electronic transition energies and not near E_1. We propose that this feature is an acoustic vibration of microcrystalline GaAs, observed via defect-assisted scattering between an electron or hole and the crystalline-amorphous interface regions characteristic of ion-implanted GaAs. The additional scattering breaks the $\mathbf{k}=0$ infinite-crystal selection rule, and double-resonance effects result in intense scattering for phonons in special regions of the Brillouin zone. Electronic wave functions with sufficiently large wavelengths (on the scale of the crystallite size) are strongly affected by the disorder. A phenomenological model accounts for the resonance behavior reasonably well.

I. INTRODUCTION

Ion implantation is a means by which disorder can be introduced into crystalline GaAs (*c*-GaAs). The damage incurred during this process results in a state intermediate to the amorphous and crystalline forms. The resulting material is a mixture of microcrystalline and amorphous GaAs, as has been substantiated by spectroscopic evidence.[1–4]

The spatial-correlation model has been successfully used to characterize the microcrystalline component of the Raman spectrum in ion implanted GaAs.[2] The physical basis for this model is that finite crystallite sizes (L) will affect long-wavelength phonons (on the scale of L). This results in a relaxation of the usual $\mathbf{k}=0$ selection rule and permits a range of phonon k values ($\Delta k \sim 1/L$) to participate in first-order Raman scattering. The resulting spectrum, for (001)-oriented GaAs starting material, exhibits a longitudinal-optical (LO) phonon which shifts down in frequency and broadens asymmetrically.

In a previous paper,[4] we have discussed measurements of the LO scattering intensity for 45-keV Be^+-implanted GaAs. The intensity of the LO line is observed to decrease with increasing ion fluence, corresponding to increased host lattice damage. The decreasing LO scattering intensity is attributed to a decrease in the optical penetration depth (scattering volume) and to a decrease in the fraction of the scattering volume which is still crystalline, as larger volume fractions of the substrate are converted to amorphous GaAs (*a*-GaAs). By varying the excitation photon energy ($\hbar\omega$) we also observed that the LO Raman-scattering intensity partially retained its resonance with the E_1 electronic interband transition. Over a photon-energy range of 1.55 to 2.2 eV the LO scattering intensity was found to depend solely upon the scattering volume. That study[4] is the first study of the photon-energy dependence of the Raman emission process in ion-implanted GaAs.

Berg and Yu[5–7] have discussed the effect that high-energy electron and neutron irradiation has on Raman and resonance-Raman processes in GaAs (both bulk and defect related). In their case, the irradiation creates high-density point defects, leaving the material primarily crystalline. Due to the deep penetration of their light particles, they probed a region of macroscopically uniform damage (homogeneous on a scale of 1000 Å or greater), even near E_0 where the optical-absorption coefficient is radically changing. They discuss resonance-Raman scattering for a variety of processes in disordered GaAs, particularly for the case of defect-assisted first-order Raman scattering.[7]

In the present work we discuss the nature of a newly observed strong feature in the Raman spectrum of ion bombarded GaAs: a relatively narrow, strongly resonant,

 ©1988 The American Physical Society

low-frequency band.[8] The intensity of this feature is strongly dependent upon the excitation photon energy. Under appropriate conditions, it is observed to be more intense than the allowed LO phonon. The physical origin of this new Raman band, which is not observed in either pure crystalline or pure amorphous GaAs, is clearly of fundamental interest. Although our experimental results do not yet appear to permit a definitive identification of the scattering mechanism, we can eliminate some possibilities and support others. We develop an interpretation of this new band based upon disorder-assisted Raman scattering. However, the exact origin of the object of our study is still open to speculation.

II. EXPERIMENT

The crystalline GaAs (*c*-GaAs) starting material was Czochralski grown, doped with chromium. (001)-oriented surfaces were cut and polished, then etched in 8:1:1 H_2SO_4:30%H_2O_2:H_2O prior to implanting to yield wafers with high optical quality. Implantation was carried out at the Texas Instruments Central Research Laboratory. 45-keV $^9Be^+$, 180-keV $^9Be^+$, or 180-keV $^{29}Si^+$ ions were implanted at room temperature 9° from (001) to reduced channeling. Fluences ranged from 10^{13} to 5×10^{14} ions/cm^2.

When used, depth profiling via chemical etch was performed using a weak 1:1:100 H_2SO_4:30%H_2O_2:H_2O etchant. Crystalline GaAs etches at a rate of approximately 530 Å/min while the damaged material etches somewhat faster, approximately 660 Å/min, as described in Ref. 4.

Room-temperature Stokes-Raman spectra were taken in a flowing-argon atmosphere. A SPEX 1403 double monochromator, along with a cooled GaAs photocathode photomultiplier in the photon-counting mode as detector, were used to measure Raman spectra. Excitation was from either a krypton- or argon-ion laser, enabling us to vary the excitation energy from 1.55 to 2.71 eV. Over this photon-energy range the optical penetration depth ($d_{\rm opt}=1/2\alpha$ for backscattering) into *c*-GaAs varies from 3900 to 260 Å.[9]

A near-backscattering geometry was employed with the laser beam incident at about 40° from the normal outside the sample (kept constant), corresponding to a maximum internal angle of 10°. LO phonon scattering is allowed in this configuration from a (001) surface; scattering by transverse-optical (TO) phonons is forbidden.[10] For light-polarization analyses, the backscattering direction is denoted $z\parallel[001]$. x and y denote the [100] and [010] directions, respectively, while $x'\parallel[110]$ and $y'\parallel[1\bar{1}0]$. Spectra shown in Figs. 1–4 were taken with the incident light polarized in the scattering plane with all polarizations collected. In order to compare Raman-scattering intensities a CaF_2 reference standard was used, as described in Ref. 4. Precision is estimated to be 10% or better.

III. OBSERVATION OF THE NEW PEAK IN THE RAMAN SPECTRUM OF ION-IMPLANTED GaAs

Figure 1 shows the variation of the Raman spectrum with 45-keV Be^+ ion implant fluence. The excitation is 1.92-eV (6471-Å) red laser light. In the crystal the $k=0$ optical-phonon selection rule is obeyed, resulting in a strong LO phonon at 292 cm^{-1}, appropriate for backscattering along a zinc-blende (001) direction. Also visible in the spectrum of the crystal is a weak TO line at 269 cm^{-1}, observed because we are not in a strict backscattering geometry and because the scattered light is collected in a cone about (001). As the implant fluence increases the LO line downshifts, broadens, and decreases in intensity. Simultaneously, the *a*-GaAs three-band continuum[11] increases in intensity and a very strong feature A near 47 cm^{-1} (full width at half maximum $=18$ cm^{-1}) is observed, which increases in intensity with fluence. No evidence of peak A is seen in the crystal, but it is evident even for the lowest fluence studied.

Figure 2 is a set of spectra, all taken from the 5×10^{14}-cm^{-2} 45-keV Be^+ implant, obtained by varying the excitation from 2.41 to 1.65 eV. At 2.41 eV the spectrum is typical of ion-damaged GaAs (Refs. 2, 4 and 12) showing the down-shifted and broaded LO and the three-band continuum characteristic of *a*-GaAs. For this spectrum, excited with green light, feature A is very weak. As the laser photon energy is decreased, two changes occur: the spectrum increases in intensity (normalized in Figs. 1–4

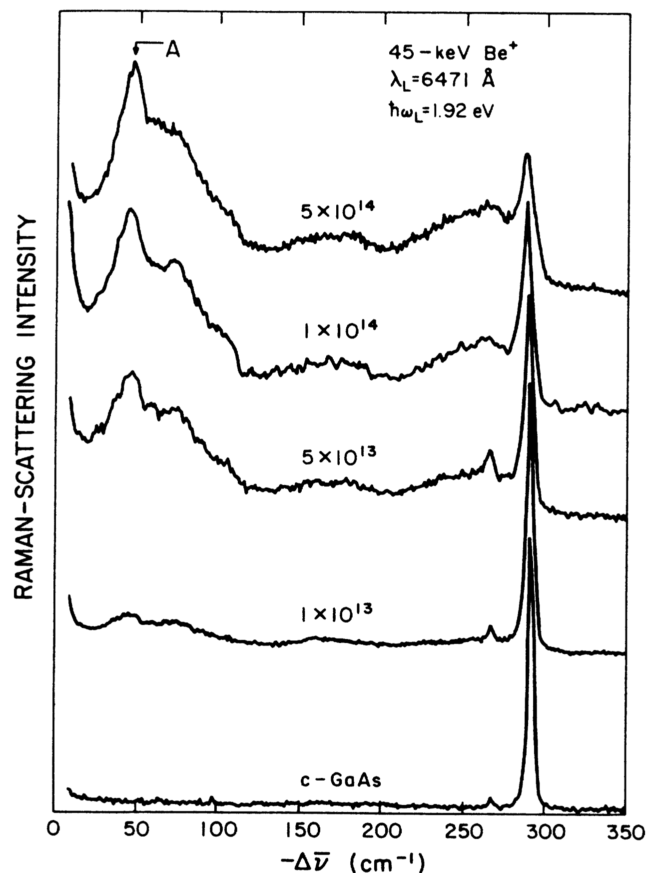

FIG. 1. Unpolarized, room-temperature Raman spectra for (100)-oriented GaAs crystals and for crystals implanted with 45-keV Be^+ ions to various fluences, measured in ions/cm^2. Excitation was with red light. Intensities are all on the same scale relative to CaF_2.

with respect to the CaF_2 standard) and the additional feature A rises above the low-energy broad band.

Previous work[2] has shown that the LO line frequency and width are characteristics of the average crystallite size present in a given implant. Detailed photon-energy dependence studies of the LO line spectra in Fig. 2 show that the LO line is not changing shape or position, indicating that between 1.65 and 2.71 eV (not shown) we are probing a range of depths having the same crystallite size distribution.[4]

The depth dependence of the Raman spectrum was studied via chemical etch removal of successive surface layers, as shown in Fig. 3. The LO line is unchanging (position, line shape, and intensity) for 0, 1, and 2 min of etch time (approximately 1500 Å), then it gradually shifts and sharpens and recovers the form of the crystalline LO line after 6 min of etching ($\sim$4000 Å), in good agreement with Ref. 4. Both the a-GaAs spectral component and the A band have intensity depth dependences complementary to that of the LO line: they are very strong near the implant surface (0–2 min);[13] then they monotonically decrease in intensity after etching beyond 2 min, becoming unobservable when the observed LO line is identical to that of the crystal. Band A does not change *shape* during this etching process, only the intensity decreases. This result is independent of the laser wavelength used, and demonstrates that the effect seen in Fig. 2 is in fact a result of changing the photon energy of the probe and not simply due to the increasing penetration depth of the light as $\hbar\omega$ is decreased.

Spectra are shown in Fig. 4 for GaAs implanted with 180-keV Be^+ (a), 180-keV Si^+ (b and d), and 45-keV Be^+ (c). The excitation source was red light. Also included (e) is the spectrum we observe with 6471-Å excitation for a flash-evaporated thin film of amorphous GaAs.[14] Since all vibrations are Raman allowed, the a-GaAs Raman spectrum resembles the full vibrational density of states (DOS) of the amorphous material,[15] it shows no sharp features anywhere.[16] On the other hand, clearly visible in all spectra of the implanted GaAs is the strong peak A at 47 cm^{-1}.

It is also noteworthy that we see no trace of the A peak in $Al_xGa_{1-x}As$ alloyed crystals. In this case the disorder-activated zone edge longitudinal-acoustic peaks in the phonon DOS (Ref. 17) were clearly observed.

In Fig. 5 polarization analyses are shown, obtained using the 1.92-eV light source. Even for these very small crystallites ($L \approx 50$ Å), the GaAs LO line retains the infinite-crystal, (001)-backscattering selection rules which are characteristic of zone-center phonons with Γ_{15} symmetry,[18] indicating that they have kept their original

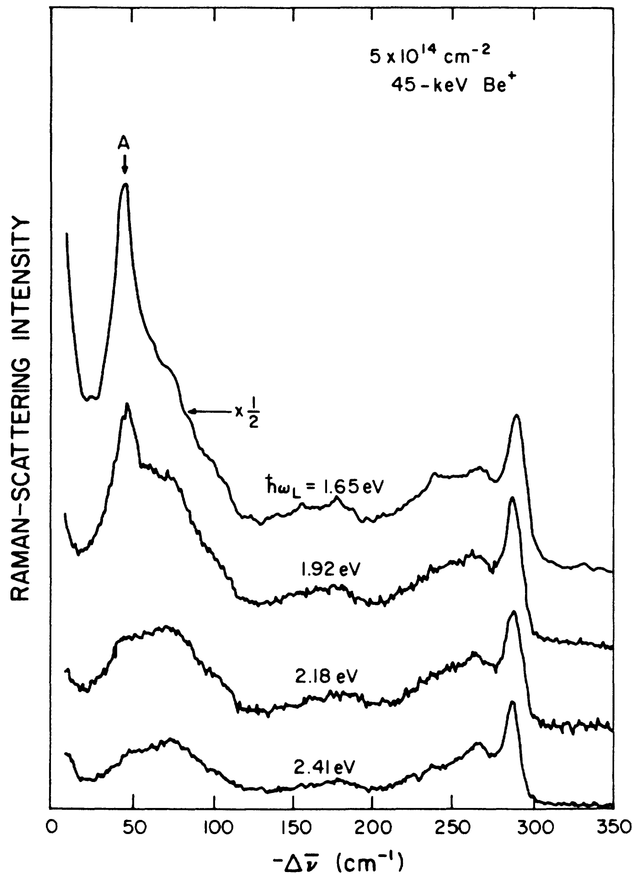

FIG. 2. Photon-energy dependence of the Raman spectrum of the 5×10-cm^{-2} 45-keV Be^+ implanted sample. The vertical scale is the same for all spectra (CaF_2 reference), except for the 1.65-eV spectrum which is scaled down by a factor of 2.

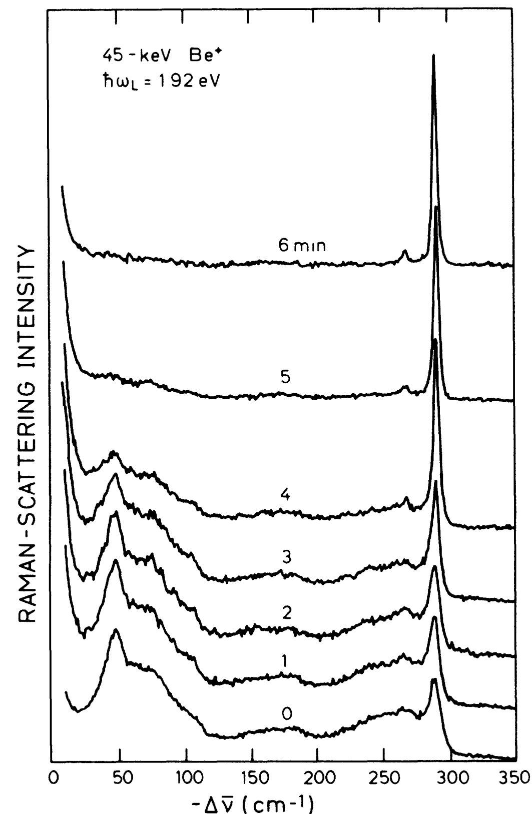

FIG. 3. Raman spectra for 45-keV Be^+-implanted GaAs following sequential chemical-etch removal of the surface layer. Etch times in minutes are noted above the data with an average etch rate of 660 Å/min. Intensities are relative to a CaF_2 standard.

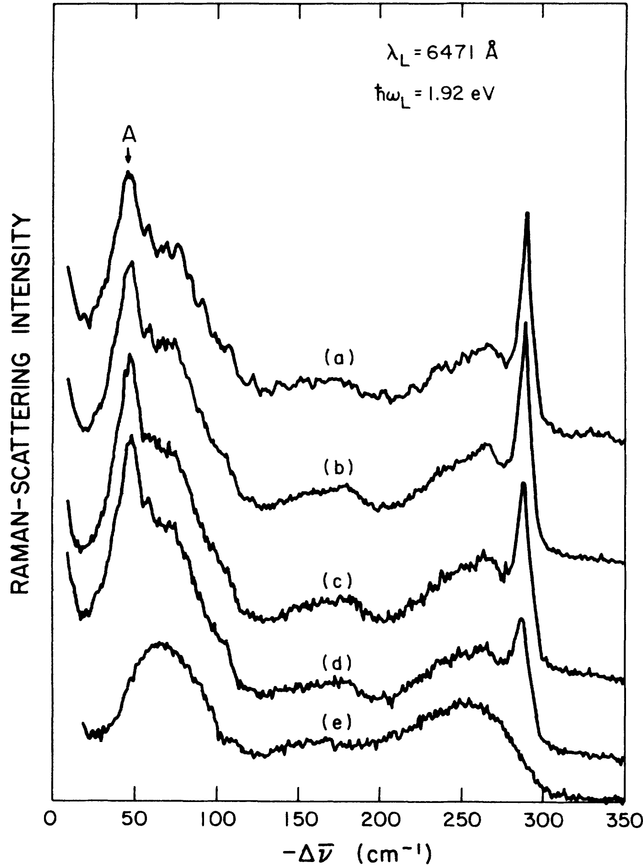

FIG. 4. Raman spectra for implanted GaAs specimens varying implant species and energies: (a) 5×10^{14}-cm^{-2} 180-keV Be^+, (b) 2×10^{13}-cm 180-keV Si^+, (c) 5×10^{14}-cm^{-2} 45-keV Be^+, and (d) 5×10^{14}-cm^{-2} 180-keV Si^+. Also (e) for amorphous GaAs. The excitation is red light. Note the strong presence of A in all spectra except for a-GaAs. Intensities for (a)–(d) are relative to CaF_2.

orientation. Amorphous GaAs has a depolarization ratio of $\sim$0.7 for the 250-cm^{-1} band.[11] Our measured results are in reasonable agreement with this. A is primarily diagonal with some $z(x,y)\bar{z}$ scattering, consistent with no zinc-blende Γ-point selection rules. Intensities are summarized in Table I. For the A band, these imply a Raman tensor with components $R_{xx}=R_{yy}=a$ and $R_{xy}=R_{yx}=b$, with a and b positive and $a/b\approx\frac{4}{3}$. The remaining entries in the 3×3 representation are undetermined. We find that $z(x',x')\bar{z}$ and $z(y',y')\bar{z}$ result in identical spectra.

IV. DEPENDENCE OF a-GaAs AND LO PHONON SCATTERING INTENSITIES ON $\hbar\omega$

In Fig. 6 we display the photon-energy dependence of I_a, the integrated intensity of the a-GaAs component (normalized to the CaF_2 standard) for the Raman spectra of three implant cases: 45-keV Be^+, 180-keV Be^+, and 180-keV Si^+ each to a fluence of 5×10^{14} cm^{-2}. Amorphous GaAs does not resonate strongly in this energy range[14] because the electronic spectrum lacks sharp structure. The measured scattering intensity should then

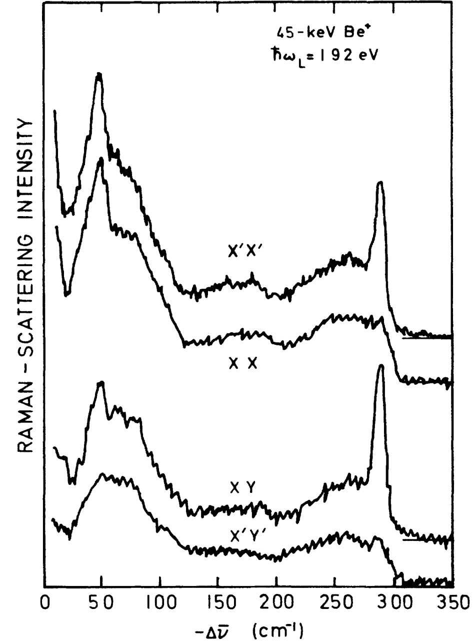

FIG. 5. Polarization analyses over the full fundamental phonon regime. Excitation is with 1.92-eV red light; intensities are arbitrary.

be a direct measure of the scattering volume. This is confirmed by the following analysis of Fig. 6.

In Ref. 4 consistent estimates for the optical-absorption coefficient were obtained on the basis of spectral evolution with etch depth, and (independently) based on LO-phonon Raman-scattering intensity measurements using a two-phase mixture of crystallites and a-GaAs. Within the mixed amorphous-microcrystalline model, the absorption coefficient is

$$\alpha=f_c\alpha_c+f_a\alpha_a \ . \tag{1}$$

The near-surface volume fractions were $f_c\approx0.75$ and $f_a\approx0.25$ for the 45-keV Be^+ case.[4] In Fig. 6 we show $1/2\alpha$ using this 75:25 mixture in Eq. (1). Photon-energy dependent α's are taken from Ref. 9 (c-GaAs) and Ref. 3 (a-GaAs). The vertical scale for the $1/2\alpha$ curve has been adjusted to fit the I_a data. Agreement for the $\hbar\omega$ dependence of I_a is good. Thus, we confirm that the measured a-GaAs intensity provides a good internal measure of the scattering volume. Normalizing other spectral components with respect to I_a thus allows us to obtain intensity values proportional to scattering efficiencies.

In Fig. 7 we implement this result for the $\hbar\omega$ dependence of I(LO), the LO line integrated intensity. I(LO) is shown, normalized to the I_a values of Fig. 6, for the same

TABLE I. Polarization of Raman spectrum main features. $\hbar\omega_L=1.92$ eV.

	$z(x,x)\bar{z}$	$z(x,y)\bar{z}$	$z(x',x')\bar{z}$	$z(x',y')\bar{z}$
LO	w	s	s	w
A	s	m	s	w
a-GaAs	s	m	s	m

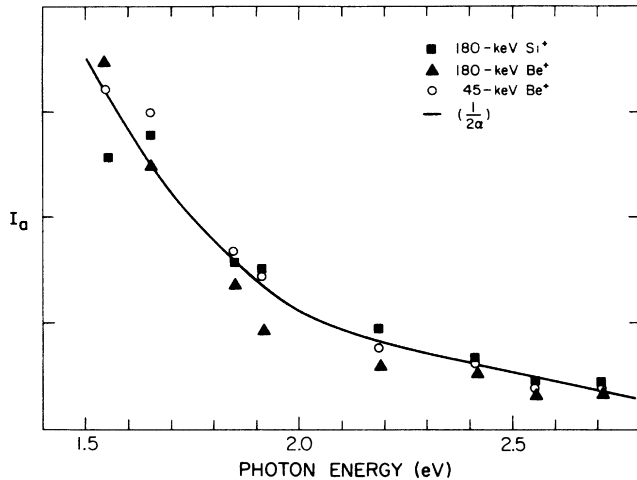

FIG. 6. Intensity measurements of the a-GaAs Raman-spectrum component (all on the same arbitrary vertical scale relative to CaF_2) vs photon energy. Each case is for a fluence of 5×10^{14} ions/cm^2, with ion species and energies shown. Data for these same three implants are shown in Figs. 6–8. The smooth curve is optical penetration depth calculated using Eq. (1), discussed in the text.

three implants of Fig. 6. For $\hbar\omega < 2.2$ eV, the LO intensity is approximately constant, exhibiting no strong resonance. For higher photon energies, the scattering efficiency is clearly increasing, indicative of resonance with the approaching E_1 interband direct electronic transition which occurs at 2.9 eV in c-GaAs.[19]

The LO line, which is present in the Raman spectrum due to the surviving crystalline component (though broadened and shifted by the effects of finite crystallite size) is expected to have a resonance spectrum similar to that seen for the bulk crystal.[7] The c-GaAs allowed TO-phonon resonance spectrum has been reported by Grimsditch *et al.*,[20] and in Fig. 7 we show their cross section (for the E_1 transitions only). The curve is scaled to agree best with the intensities measured for 180-keV Be-implanted GaAs, which possesses the largest crystallites and crystalline volume fraction of the three cases presented. Thus, the stronger resonance at high photon energies is consistent with the lower damage: it is closest to the bulk crystal. The other two implants shown in Fig. 7 have resonances which are diminished in strength to a greater extent. The curve shown can be made to fit the less-resonant data via a simple rescaling, implying resonance with the same features in the GaAs electronic structure.

The general agreement between the LO scattering intensity data and the bulk TO phonon scattering of Ref. 20 confirms that allowed features which arise from the crystalline volume fraction, and which correspond to allowed Raman-active modes in the crystal, resonate with the electronic structure in a manner similar to allowed resonances in the parent material. Particularly relevant to the present topic is that the LO line is strongly resonating at the high end of our photon-energy range, and is not resonating between 1.55 and 2.2 eV.

V. RESONANCE OF THE A PEAK NEAR E_0

In Fig. 8 $I(A)$, the integrated intensity of peak A, is exhibited (normalized to I_a) for the same implants shown in Figs. 6 and 7, over the same energy range. As can be seen in this figure (as well as directly from the data in Fig. 2), the scattering efficiency of A rapidly rises as $\hbar\omega$ decreases, it peaks between 1.6 and 1.8 eV, then decreases at 1.55 eV. Note that this strong variation in $I(A)/I_a$ affirms that A does not originate from the amorphous portion of the implanted GaAs.

To convince ourselves that we are probing only the uniformly damaged surface regions of these implanted samples, we first studied the most deeply damaged case: 180-keV Be^+ implants. Via chemical etching, we observed the damage plateau to extend from the surface to at least 5000 Å, which is larger than $d_{opt} = 3900$ Å for 1.55-eV light in c-GaAs.[9] Thus, in this case we probe uniformly damaged volumes across the full photon-energy range used.

Constant damage volumes were probed in all three cases shown in Figs. 6–8. This was confirmed by careful-

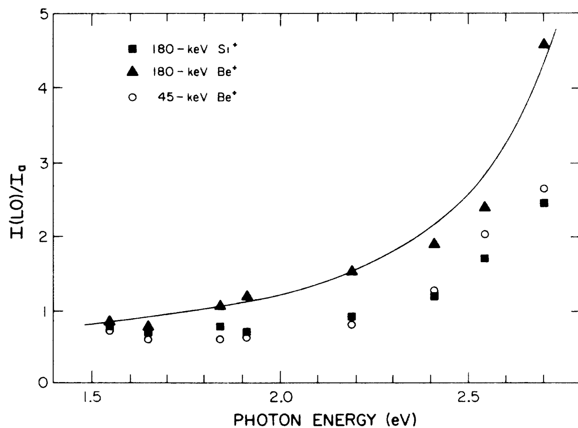

FIG. 7. Photon-energy dependence of the LO band integrated intensities (normalized to I_a in Fig. 6). The curve is from Ref. 20 for resonance with E_1 only.

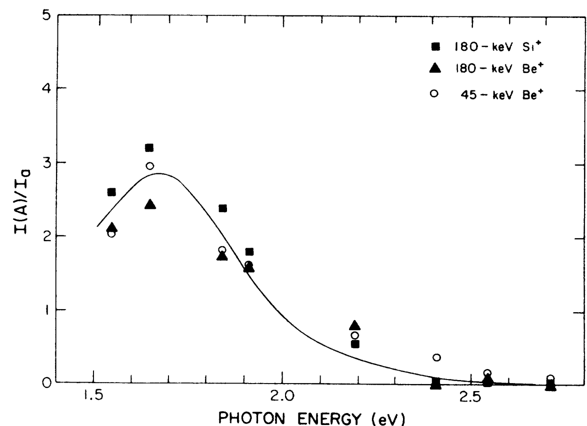

FIG. 8. Intensity of band A, relative to I_a, vs excitation energy. Figures 7 and 8 are on the same scale and exhibit completely different resonances. The curve is discussed in the text.

ly analyzing the LO line shape between 1.55 and 2.71 eV, which provides us with a sensitive gauge of the damage extent. If we probe substantially beyond the damage plateau (by decreasing $\hbar\omega$), the LO line will sharpen and shift to higher energy. The frequencies and line shapes were found to be constant over our $\hbar\omega$ range.[21] We thereby confirm nondestructively that the data shown in Figs. 6–8 are for regions of macroscopically uniform damage in GaAs. The decreases in $I(A)/I_a$ at 1.55 eV in Fig. 8, and consequently the peaks observed in all three data sets, are believed to be real, and the general agreement for these three cases supports this viewpoint.

The results presented in Fig. 8 are interpreted as strong evidence of a resonance in A at an energy midway between the c-GaAs E_0 and $E_0+\Delta_0$ interband electronic transitions at 1.43 and 1.77 eV, respectively.[22] In the absence of resonance effects, both Figs. 7 and 8 would be flat curves. The density of data points presented does not permit us to pinpoint the photon energy at which A has maximum intensity, but identification of the mechanism responsible for A must be in accord with Fig. 8 and the general nature of the resonance exhibited here.

Reflectance measurements of c-GaAs and Be-implanted GaAs are shown in Fig. 9. Clearly resolved for the c-GaAs are the peaks corresponding to the E_1 and $E_1+\Delta_1$ peaks in the electronic DOS (2.9 and 3.1 eV, respectively). In the implanted spectrum these peaks merge into a single, broad feature, accompanied by a weak overall shift to higher energies. It is not unreasonable to expect that the E_0 and $E_0+\Delta_0$ transitions are similarly affected. The peak in the DOS would occur at an energy, E_c, near the average energy with a bandwidth $\eta \approx \Delta_0$. The DOS maxima may thus broaden and shift with damage.

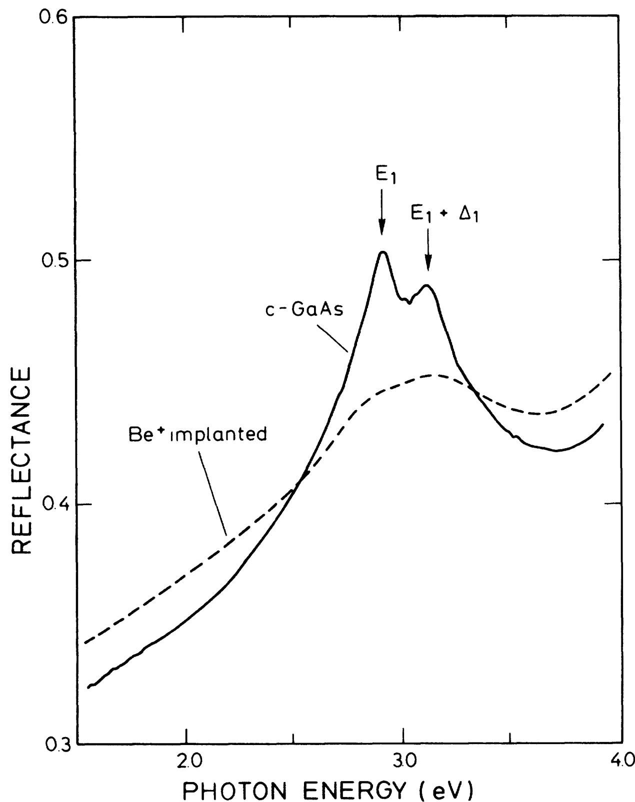

FIG. 9. Room-temperature reflectance measurements for c-GaAs before and after implanted with 45-keV Be^+ ions to a fluence of 5×10^{14} cm^{-2}.

In the photon-energy range where the LO line is not resonating, it also is a measure of the light-scattering volume. For 1.92-eV light, we observe that $I(A)/I(\mathrm{LO}) \sim L^{-1}$, where the crystallite sizes (L values) have been obtained from the LO peak frequencies and line widths. It is interesting to note that if $I(\mathrm{LO}) \sim L^3$ (crystallite volume) then $I(A) \sim L^2$ (crystallite surface area). This is evidence that A is in some way associated with the crystalline-amorphous interface regions.

VI. BRIEF SYNOPSIS OF THE EXPERIMENTAL FINDINGS ABOUT PEAK A

Thus far, we have presented data pertaining to the new feature A. The studies have included data over a wide range of implant fluences, with various ion energies and species. The experimental results are summarized as follows.

(1) A strong feature is observed in the Raman spectrum of ion-implanted GaAs.

(2) It has constant line shape, is fairly narrow, and the frequency shifts very little over the large range of damage studied.

(3) It is absent in c-GaAs.

(4) It is absent in a-GaAs.

(5) It is absent in $Al_xGa_{1-x}As$ alloys.

(6) The intensity depth profile of the new feature within the damage layer is the same as the a-GaAs spectral-component intensity and complementary to that of the LO line.

(7) It is strongly resonant near the broadened E_0 interband transition, which is in strong contrast to the crystalline allowed LO line, which resonates near E_1.

(8) $I(A)/I(\mathrm{LO}) \sim L^{-1}$ for $\hbar\omega = 1.92$ eV.

VII. DISCUSSION OF THE ORIGIN OF THE NEW FEATURE

It is useful to list hypothetical explanations for the origin of the new band. (i) Maxima in the vibrational DOS, including microcrystallite size effects; (ii) zone-folded Raman-active acoustical vibrations; (iii) impurity-specific vibrations or electronic levels; (iv) damage-induced native defects or single phases; (v) crystallite surface modes; (vi) vibrations specific to the crystal-amorphous interface region; and (vii) defect-assisted scattering of GaAs acoustic phonons.

Let us discuss the expected nature of each of these in light of the experimental results presented. (i) The frequency of A lies in the range of acoustical vibrations in c-GaAs.[23] The lowest-frequency critical point in the phonon DOS is the transverse-acoustic (TA) band at the L

point in the Brillouin zone (BZ), $\omega_{TA}(L)=60$ cm^{-1}. For small enough crystallite size periodic boundary conditions no longer apply, which affects the phonon DOS.[24] This leads to modifications in the DOS which are strongly dependent on the crystallite size. We do not observe this effect in A: the frequency does not vary significantly for various implant cases, corresponding to widely different crystallite sizes (the range of crystallite diameters in Fig. 1 is from 300 to 50 Å for fluences 1×10^{13} and 5×10^{14} cm^{-2}, respectively[2,4]). If A is an intrinsic c-GaAs vibration, then $0<k_A<k_{BZ}$.

(ii) Zone folding has been observed to activate non-zone-center acoustic phonons in both crystalline $GaAs/Ga_xAl_{1-x}As$ heterostructures[25] and in amorphous heterostructures.[26] While we do not have repeat-distance order in our implanted GaAs, vibrational features may be affected by the apparently consistent texture of the scattering medium, but only in a statistical sense. However, such zone-folded Raman-active acoustic modes have frequencies which vary with the quantum-well period, resulting in difficulties for (ii).

Impurity-specific vibrations (iii) are clearly eliminated by the fact that we observe A in different implants. Similarly, electronic-Raman scattering[27] is not responsible for the A peak since it is present for different implant species. Furthermore, our experiments were carried out at room temperature which causes such shallow impurity levels to be unresolved from the host semiconductor electronic levels.

Native defects (iv) resulting from the ion damage (e.g., interstitials, vacancies, antisites, etc.) are expected to be in high density. However, the low frequency of the A band, well within the fundamental phonon regime of GaAs, serves as an argument against assigning it to a defect mode. Decay into GaAs fundamental modes would delocalize specific defect vibrations, broadening them beyond recognition (especially at room temperature). In contrast, we observe a well-defined peak.

Single-phase arsenic (either amorphous or crystalline), present from either the implant process or caused by laser heating, is not the origin of A. This is clear from the fact that we see no strong bands near 200 and 225 cm^{-1} (crystalline As), 220 and 255 cm^{-1} (orthorhombic As), or broad bands in the 200–240 cm^{-1} range (amorphous As).[28]

The observation of a spectral feature present only in the characteristic mixed amorphous-microcrystalline ion-implanted material, but absent in either pure c-GaAs or a-GaAs, suggests a mechanism that involves the crystallite surfaces (v) or crystal-amorphous interface regions (vi). Vibrational modes attributed to such interface regions have several attractive features for our purposes: the frequency would be constant and their number would increase in proportion to the internal surface area $S/V\sim L^{-1}$. Over nearly 1 order of magnitude we observe that $I(A)/I_{LO}\sim L^{-1}$, with approximate crystallite sizes obtained from the LO line.[2] However, such modes have the same degeneracy with the fundamental vibrations as (iv), and would therefore be quite broad.

We do not expect symmetry to play a strong role in the resonance of these features because long-wavelength excitations (i.e., near the Γ point) will experience strong interactions with the disorder: long-range symmetry becomes less imposing with smaller crystallite size. Crystallite-size effects, such as the phonon-confinement mechanism which well describes the LO-phonon line-shape behavior, are not sufficient to account for the A band. For the LO phonon, decreasing crystallite size permits a larger range of $\mathbf{k}$ values (around $\mathbf{k}=0$) to participate in first-order Raman scattering. The LO band downshifts and broadens on account of the weak negative dispersion of the LO branch. For acoustic vibrations, the dispersion is steep near $\mathbf{k}=0$, making the corresponding upshift with decreasing L quite large. This is not observed.

VIII. DEFECT-ASSISTED RAMAN SCATTERING OF GaAs ACOUSTIC PHONONS

Critical findings are observations of the resonance behavior of A, and the great difference between this resonance and that exhibited by the allowed LO line. A resonates near E_0 and *not* near E_1. The LO line resonates near E_1 and *not* near E_0. The LO-phonon Raman resonance is well accounted for in terms of the relative $\mathbf{k}$-space volumes involved.

Perhaps the large spatial extent of the electronic wave functions are a requirement for the effect we observe. Electrons with short wavelengths will not be strongly affected by the crystallite size. For $\hbar\omega<2.2$ eV the uppermost valence bands and lowest conduction band,[29] near the E_0 and $E_0+\Delta_0$ peaks in the DOS, which are responsible for the overall optical properties in this energy regime, require that $|\mathbf{k}|<0.2k_{BZ}$ ($\lambda>10a_0$). For the E_1 transition $|\mathbf{k}|>0.3k_{BZ}$. Hence, wave functions for electrons near the Γ point in the Brillouin zone would be strongly influenced by the small crystallite nature of the disorder.

We therefore propose a mechanism for the strong scattering of GaAs acoustic phonons via a defect-assisted Raman-scattering mechanism (vii). The "defects" in this case are the microcrystal-amorphous interface, or "surface" regions, which are present in implanted GaAs but absent in either crystalline or amorphous GaAs. Because the disordered material has a much lower electronic mobility, photoexcited electrons will not readily travel from the microcrystallites into the a-GaAs. Thus, the interface elastically scatters electrons, resulting in a momentum transfer. This transfer of momentum results in a breakdown of the $\mathbf{k}=0$ infinite-crystal selection rule, permitting the electron to participate in single-phonon Raman scattering with nonzone-center phonons. Double-resonance effects then give rise to intense scattering from distinct regions within the Brillouin zone (away from $\mathbf{k}=0$).

A prominent defect-assisted scattering analysis derives from two-phonon scattering by replacing one of the electron-phonon[30] interactions with an elastic electron-defect collision.[31] This additional event acts to alter the electronic $\mathbf{k}$ vector, relaxing the strict $\mathbf{k}$ selection rules imposed by long-range crystalline order. The scattering process therefore consists of fourth-order perturbation

terms involving electron-phonon and electron-defect interactions, along with the usual photon absorption and emission.

Following the summary of the treatment by Berg and Yu,[7] the defect-assisted scattering is developed considering only two-band processes with parabolic bands. Excitonic effects are ignored and the Born approximation is used. Scattering cross sections then take on the (intrinsic scattering) form

$$\sigma(\omega_L)\sim \int_{BZ} q^2 dq\, |f(q,\omega_L\omega_S)A_T(q,\omega_L)|^2 , \quad (2)$$

where f is a function which accounts for the specific mechanisms involved[32] in the electron-phonon scattering (e.g., deformation potential) and in the electron-defect interaction. The function A_T (see the Appendix) accounts for the scattering processes involved in this fourth-order perturbation expansion. The primary physical quantities for the model are m_e, the electron effective masses; E_c, the critical-point energy; and η, the width of the E_c transition. The cross section in Eq. (3) may then be approximated numerically, once the scattering mechanisms f have been identified.

Menendez and Cardona[33] observed impurity-assisted forbidden LO phonon scattering (Fröhlich) near $E_0+\Delta_0$ in GaAs. The dopant impurities were allowed to interact with the electrons (holes) via a screened-Coulomb potential where k_F, the screening wave vector, is determined by the mean distance between defects. The LO phonon scattering was via the Fröhlich mechanism introducing an additional $1/k$ factor. The additional scattering event caused the system to show double-resonance effects with the largest contribution to the scattering intensity coming from phonons with $k \approx 0.2/a_0$ (a_0 is the lattice constant). Calculated results were in good agreement with the experiment. Of particular interest is the fact that strong double-resonance effects were seen for phonons with k large compared to k_F and k large compared to $k_i = 2\pi n(\lambda_L)/\lambda_L + 2\pi n(\lambda_s)/\lambda_s$, the (backscattering) wave vector required for zone-center Raman scattering.

Berg and Yu[7] extended the results of Menendez and Cardona to the case of a variety of defects in electron- and neutron-irradiated GaAs. They discuss the generalization of the fourth-order scattering process near E_0. For defect vibrations which may be treated as local modes they find that double-resonance scattering comes primarily from a narrow range of k values around $0.1/a_0$.

In the cases of defect-assisted Raman scattering cited above, the vibrations were considered to be dispersionless. Taking the A band as resulting from intrinsic c-GaAs vibrations requires that they be acoustic vibrations. Zone-center acoustic vibrations have Γ_{15} symmetry in the zinc-blende crystal structure.[10] Group compatibility tables along the symmetry directions[34] indicate that acoustic vibrations with k between Γ and X points in the Brillouin zone have Raman tensors consistent with our determination for peak A. However, the caveat of selection-rule breakdown near resonance weakens the implication. For scattering involving acoustic phonons, frequencies change radically over the Brillouin zone. Their dispersion must therefore be accounted for when considering scattering by acoustic phonons. This is done by using the measured dispersion.[23]

The electron-defect interaction responsible for the observed effect, for which it is proposed that the electronic wave-function wavelength is an important parameter, must be sufficiently general to explain the observation of A in all implants studied. The view taken here is that the defects are the amorphous-crystalline interface regions. Electronic wave functions are assumed to be backscattered in an infinite-potential barrier manner. It is sufficient, in this analysis, to simply impose this elastic scattering, which serves only to alter the electronic wave vector, thereby breaking the $k=0$ restriction.

In Fig. 8 we show a two-band resonance-Raman cross section calculated using Eq. (2). The curve is for a merged E_0 and $E_0+\Delta_0$ case, with $E_c = 1.65$ eV and $\eta = 0.4$ eV to best agree with the data. The electron-phonon scattering is via the deformation potential.[35] Equation (2) then becomes

$$\sigma(\omega_L)\sim \left| \int \frac{q^3 dq}{\sqrt{\omega(q)}} A_T(q,\omega_L) \right|^2 \quad (3)$$

where integration is carried out first (extrinsic). The resulting σ was insensitive to the order of integration of squaring. Parameters used in evaluating Eq. (3) are from Ref. 22.

The 1.65-eV critical-point energy, found to best agree with the data in Fig. 8, does not precisely correspond to the weighted average energy for E_0 transitions ($E_0+\Delta_0/3 = 1.53$ eV). Since reflectance measurements show nothing in this energy range and absorption measurements are difficult, there are no concurring measurements for our proposed merged-band picture.

Various scattering scenarios were considered with less success. It is important to note that critical-point energy widths closer to the crystalline η values (near 0.1 eV, Ref. 36) result in sharp cross sections. This is in contrast to A which is relatively broad.

Agreement between the calculated cross section and the data is only satisfactory. The primary contribution to the scattering comes from $k \approx 0.1 k_{BZ}$ implicating consistency between the frequency of A and the acoustic bands of GaAs.[23] Similar agreement is found when considering electron-acoustic phonon scattering via the piezoelectric effect. Since GaAs is weakly piezoelectric, the deformation potential is more plausible. In any case, we find some consistency between the data and the model.

IX. SUMMARY

We have observed a strong, resonant feature (A) in the room-temperature Raman spectrum of ion-implanted GaAs (Figs. 1–5), prior to any anneal. It is observed over a wide range of implant conditions (species, energies, and fluences), but it is not observed in either the crystalline or amorphous phases. The feature is strong for excitation photon energies below 2.2 eV; above 2.2 eV it is weak and is masked by the a-GaAs component of the spectrum. The frequency and line shape vary little.

Careful intensity measurements of the a-GaAs component of the Raman spectrum, I_a, relative to CaF_2, indicate that it depends solely upon optical penetration depth (Fig. 6). I_a then provides us with an *internal* standard for optical penetration over the full photon-energy range studied (1.55–2.71 eV). Thus, scattering volume effects and scattering efficiencies may be separated.

Based upon this, the LO line of the microcrystalline remnant is seen to resonate with the approaching E_1 interband electronic transition near 3 eV (Fig. 7), and not with the E_0 transition critical points in the density of states. The resonance is similar to reported allowed-TO measurements on c-GaAs,[20] as expected for features arising from the crystalline component of the implanted material.

A is seen to resonate somewhere between E_0 and $E_0+\Delta_0$, but not near E_1 (Fig. 8). A is seen strongly for $\hbar\omega_L < 2.2$ eV which corresponds to $k < 0.2k_{BZ}$ for photon absorption between the uppermost valence and lowest conduction bands of GaAs. This implies that only electrons with sufficiently large wavelengths, on the scale of the microcrystallite dimensions, are affected by the disorder, and may thereby participate in the scattering process responsible for A. Hence the large-k electronic wave functions, primarily responsible for photon absorption near the E_1 transition, are not strongly influenced by the microcrystallinity, and for this reason do not have a strong scattering cross section.

We propose that defect-induced Raman scattering by acoustic modes of GaAs is responsible for the new feature. The defects are taken to be simply the interface regions between the GaAs crystallites and the amorphous GaAs. The electron scatters elastically from the low-mobility a-GaAs (and is thereby restricted to the crystalline component), resulting in a momentum transfer which breaks the $k=0$ selection rule. The scattering cross section is large when double-resonance conditions are satisfied. A model, developed to account for this type of process in the presence of point defects,[7,33] is adapted to the present case, with some success.

ACKNOWLEDGMENTS

The authors are indebted to A. Purdes and S. Matteson of the Texas Instruments Central Research Laboratory for providing the implanted GaAs materials used in this study. We also thank J. Cunningham of AT&T Bell Laboratories for providing the $Al_xGa_{1-x}As$ alloy. Helpful discussions with G. Feng and S. Holtz are acknowledged, along with the assistance of G. Feng in collecting the reflectance data. This work was supported by Texas Instruments and the Virginia Center for Innovative Technology.

APPENDIX

Definitions of the function A_T for the defect-assisted Raman scattering process from Ref. 7 as follows:

$$\begin{aligned} A_T(\omega_L) = {} & A(s_e x, -s_e x, x_1, x_2, x_3) + A(s_h x, -s_h x, x_1, x_2, x_3) - A(s_e x, s_h x, x_1, x_2, x_3) \\ & - A(s_h x, s_e x, x_1, x_2, x_3) + A(s_e x, -s_e x, x_1, x_2', x_3) + A(s_h x, -s_h x, x_1, x_2', x_3) \\ & - A(s_e x, s_h x, x_1, x_2', x_3) - A(s_h x, s_e x, x_1, x_2', x_3)\,, \end{aligned} \tag{A1}$$

where

$$\begin{aligned} A(\lambda_1\mathbf{q},\lambda_2\mathbf{q},k_1,k_2,k_3) = {} & \frac{\lambda_1}{\lambda_1+\lambda_2} A(0,\lambda_1\mathbf{q},S^{1/2},k_2,k_1) \\ & + \frac{\lambda_2}{\lambda_1+\lambda_2} \times A(0,\lambda_2\mathbf{q},S^{1/2},k_2,k_3)\,, \end{aligned} \tag{A2}$$

$$A(0,\lambda_j\mathbf{q},k_1,k_2,k_3) = \frac{16\pi^2}{(k_1^2-k_2^2)\lambda_j q} \times \left[\tan^{-1}\left[\frac{i\lambda_j q}{k_1+k_3}\right] - \tan^{-1}\left[\frac{i\lambda_j q}{k_2+k_3}\right] \right], \tag{A3}$$

$$x = aq,\quad x_j = ak_j,\quad x_2' = ak_2',\quad a = \left[\frac{\hbar^2}{2\mu\hbar\omega_{\mathrm{LO}}}\right]^{1/2}, \tag{A4}$$

$$k_j = \left[\frac{2\mu}{\hbar^2}\left[\hbar\omega_L + i\eta - E_c - (j-1)\hbar\omega_p - \delta_{j,2}\frac{\hbar^2 q^2}{2M}\right]\right]^{1/2} \quad (j=1,2)\,, \tag{A5}$$

$$k_3 = \left[\frac{2\mu}{\hbar^2}(\hbar\omega_L + i\eta - E_c - \hbar\omega_p)\right]^{1/2}, \quad \mathrm{Im}(k_3) > 0 \tag{A6}$$

$$k_2' = \left[\frac{2\mu}{\hbar^2}\left[\hbar\omega_L + i\eta - E_c - \frac{\hbar^2 q^2}{2M}\right]\right]^{1/2}, \quad \mathrm{Im}(k_2') > 0 \tag{A7}$$

$$M = m_e + m_h,\quad s_{e,h} = m_{e,h}/M,\quad \frac{1}{\mu} = \frac{1}{m_e} + \frac{1}{m_h}\,, \tag{A8}$$

$$S = \frac{\lambda_1 k_3^2 + \lambda_2 k_1^2}{\lambda_1+\lambda_2} - \lambda_1\lambda_2 q^2\,. \tag{A9}$$

*Present address: Max-Planck-Institut FKF, D-7000 Stuttgart 80, Federal Republic of Germany.

[1]D. E. Aspnes, S. M. Kelso, C. G. Olson, and D. W. Lynch, Phys. Rev. Lett. **48**, 1863 (1982).

[2]K. K. Tiong, P. M. Amirtharaj, F. H. Pollak, and D. E. Aspnes, Appl. Phys. Lett. **44**, 122 (1984).

[3]J. B. Theeten and M. Erman, J. Vac. Sci. Technol. **20**, 471 (1982).

[4]M. Holtz, R. Zallen, O. Brafman, and S. Matteson, Phys. Rev. B **37**, 4609 (1988).

[5]R. S. Berg, P. Y Yu, and E. R. Weber, Appl. Phys. Lett. **47**, 515 (1985).

[6]R. S. Berg and P. Y. Yu, Phys. Rev. B **33**, 7349 (1986).

[7]R. S. Berg and P. Y. Yu, Phys. Rev. B **35**, 2205 (1987).

[8]M. Holtz, R. Zallen, and O. Brafman, Phys. Rev. B **37**, 2737 (1988).

[9]D. E. Aspnes and A. A. Studna, Phys. Rev. B **27**, 985 (1983).

[10]W. Hayes and R. Loudon, *Scattering of Light by Crystals* (Wiley, New York, 1978).

[11]R. Zallen, M. Holtz, R. Sadler, and A. Geissberger, Bull. Am. Soc. Phys. **31**, 476 (1986).

[12]T. Nakamura and T. Katoda, J. Appl. Phys. **53**, 5870 (1982).

[13]Etched samples exhibit stronger parasitic scattering, which must be taken into consideration when comparing intensities in the low-frequency range.

[14]Flash-evaporated *a*-GaAs thin films were provided by M.-L. Theye of the Université Pierre et Marie Curie, Paris; M.-L. Theye and A. Gheorghiu, Sol. Energy Mater. **8**, 331 (1982).

[15]R. Zallen, *The Physics of Amorphous Solids* (Wiley, New York, 1983).

[16]The *A* peak is not observed in implant-amorphized GaAs, Ref. 11.

[17]H. Kawamura, R. Tsu, and L. Esaki, Phys. Rev. Lett. **29**, 1397 (1972).

[18]M. Cardona, in *Light Scattering in Semiconductors,* Vol. 2 of *Topics in Applied Physics,* edited by M. Cardona and G. Güntherodt (Springer, Berlin, 1982), p. 49.

[19]H. Ehrenreich, H. R. Philipp, and J. C. Phillips, Phys. Rev. Lett. **8**, 59 (1962).

[20]M. H. Grimsditch, D. Olego, and M. Cardona, Phys. Rev. B **20**, 1758 (1979).

[21]M. Holtz, Ph.D. thesis, Virginia Tech, 1987.

[22]J. S. Blakemore, J. Appl. Phys. **53**, R123 (1982).

[23]J. L. T. Waugh and G. Dolling, Phys. Rev. **132**, 2410 (1963); B. Dorner and D. Strauch (private communication).

[24]R. K. Pathria, *Statistical Mechanics* (Pergamon, Oxford, 1972), p. 487.

[25]C. Colvard, R. Merlin, M. V. Klein, and A. C. Gossard, Phys. Rev. Lett. **45**, 289 (1980); C. Colvard, T. A. Gant, M. V. Klein, R. Merlin, R. Fischer, H. Morkoç, and A. C. Gossard, Phys. Rev. B **31**, 2080 (1985).

[26]P. Santos, M. Hundhausen, and L. Ley, Phys. Rev. B **33**, 1516 (1986).

[27]K. Wan and R. Bray, Phys. Rev. B **32**, 5265 (1985).

[28]J. S. Lannin, J. M. Calleja, and M. Cardona, Phys. Rev. B **12**, 585 (1975); J. S. Lannin, *ibid.* **15**, 3863 (1977); J. S. Lannin and B. V. Shanabrook, in *Proceedings of the 14th International Conference on the Physics of Semiconductors,* IOP Conf. Proc. Ser. No. 43, edited by B. Wilson (IOP, London, 1978), p. 643.

[29]M. L. Cohen and J. R. Chelikowsky, in *Handbook on Semiconductors,* edited by W. Paul (North-Holland, Amsterdam, 1982).

[30]Holes also contribute to the net scattering cross section.

[31]A. G. Gogolin and E. I. Rashba, Solid State Commun. **19**, 1177 (1976).

[32]In Eq. (2) the contributions to the scattering cross section have been squared then integrated over **k** space, appropriate for intrinsic scattering mechanisms. For extrinsic scattering, integration must be performed first (reconstructing the **k**-space contributions for scattering involving components from the entire Brillouin zone), then the result is squared.

[33]J. Menendez and M. Cardona, Phys. Rev. B **31**, 3696 (1985).

[34]R. H. Parmenter, Phys. Rev. **100**, 573 (1955).

[35]G. Mahan, *Many Particle Physics* (Plenum, New York, 1981), p. 38.

[36]S. Gopalan, P. Lautenschlager, and M. Cardona, Phys. Rev. B **35**, 5577 (1987).